
Fast Locality Sensitive Hashing with Theoretical Guarantee

Zongyuan Tan^{*1} Hongya Wang^{*1} Bo Xu¹ Minjie Luo² Ming Du¹

Abstract

Locality-sensitive hashing (LSH) is an effective randomized technique widely used in many machine learning tasks. The cost of hashing is proportional to data dimensions, and thus often the performance bottleneck when dimensionality is high and the number of hash functions involved is large. Surprisingly, however, little work has been done to improve the efficiency of LSH computation. In this paper, we design a simple yet efficient LSH scheme, named FastLSH, under l_2 norm. By combining random sampling and random projection, FastLSH reduces the time complexity from $O(n)$ to $O(m)$ ($m < n$), where n is the data dimensionality and m is the number of sampled dimensions. Moreover, FastLSH has provable LSH property, which distinguishes it from the non-LSH fast sketches. We conduct comprehensive experiments over a collection of real and synthetic datasets for the nearest neighbor search task. Experimental results demonstrate that FastLSH is *on par with* the state-of-the-arts in terms of answer quality, space occupation and query efficiency, while enjoying up to 80x speedup in hash function evaluation. We believe that FastLSH is a promising alternative to the classic LSH scheme.

1. Introduction

Nearest neighbor search (NNS) is an essential problem in machine learning, which has numerous applications such as face recognition, information retrieval and duplicate detection. The purpose of nearest neighbor search is to find the point in the dataset $\mathbf{D} = \{v_1, v_2, \dots, v_N\}$ that is most similar (has minimal distance) to the given query u . For low dimensional spaces (< 10), popular tree-based index structures such as KD-tree (Bentley, 1975), SR-tree (Katayama

& Satoh, 1997), etc. deliver exact answers and provide satisfactory performance. For high dimensional spaces, however, these index structures suffer from the well-known curse of dimensionality, that is, their performance is even worse than that of linear scans (Samet, 2006). To address this issue, one feasible way is to offer approximate results by trading accuracy for efficiency (Kushilevitz et al., 1998).

Locality-sensitive hashing (LSH) is an effective randomized technique to solve the problem of approximate nearest neighbor (ANN) search in high dimensional spaces (Indyk & Motwani, 1998; Datar et al., 2004; Andoni & Indyk, 2008). The basic idea of LSH is to map high dimensional points into buckets in low dimensional spaces using random hash functions, by which similar points have higher probability to end up in the same bucket than dissimilar points. A number of LSH functions are proposed for different similarity (distance) measures such as Hamming distance (Indyk & Motwani, 1998), l_2 norm (Datar et al., 2004), angular similarity (Charikar, 2002), Jaccard similarity (Shrivastava, 2017) and maximum inner product (Shrivastava & Li, 2014a).

The LSH scheme for l_2 norm (E2LSH) is originally proposed in (Datar et al., 2004; Andoni, 2005) based on p -stable distributions. Owing to the sub-linear time complexity and theoretical guarantee on query accuracy, E2LSH is arguably one of the most popular ANN search algorithms both in theory and practice, and many variants have been proposed to achieve much better space occupation and query response time (Lv et al., 2007; Tao et al., 2010; Gan et al., 2012; Sun et al., 2014; Huang et al., 2015; Lu & Kudo, 2020; Yang et al., 2020; Zheng et al., 2020; Tian et al., 2022). Throughout this article, we focus on the LSH scheme under l_2 norm, and the extension for angular similarity and maximum inner product will be discussed in Section 5.

In addition to answer ANN queries, LSH finds applications in many other domains. To name a few, LSH is utilized in hierarchical clustering to approximate the distances and reduce the time complexity of clustering (Koga et al., 2007). (Chen et al., 2011) uses LSH to remove outliers from the initial samples in order to perform association rule mining on large datasets in a reasonable amount of time. Recently, LSH is recognized as an effective sampler for efficient large-scale neural network training (Chen et al., 2020).

^{*}Equal contribution ¹School of Computer Science and Technology, Donghua University, Shanghai, China ²College of Science, Donghua University, Shanghai, China. Correspondence to: Hongya Wang <hywang@dhu.edu.cn>.

All of these LSH applications involve computation of LSH functions over the entire dataset. Take the widely used E2LSH as an example, computing k hashes of a vector \mathbf{v} takes $O(nk)$ computation, where n is the dimensionality of \mathbf{v} and k is the number of hash functions. For typical ANN search task, k commonly ranges from few hundreds to several thousands, and keeps growing with the cardinality of the dataset (N) since the number of hashes required by E2LSH is $O(N^\rho)$ (Datar et al., 2004). Hence, hashing is the main computational and resource bottleneck step in almost all LSH-based applications, especially when data come in a streaming fashion and/or LSH data structures have to be constructed repeatedly (Yang et al., 2020; Sundaram et al., 2013).

One notable work for speeding up the computation of LSH functions is the densified one permutation hashing (Shrivastava & Li, 2014b), which requires only $O(n+k)$ computations instead of $O(nk)$ of Minhashing (Shrivastava, 2017). Surprisingly enough, little endeavor has been made on more efficient LSH schemes under l_2 norm. The only known technique, termed as ACHash (Dasgupta et al., 2011), exploits fast Hadamard transform to estimate the distance distortion of two points in the Euclidean space. This method, like other fast JL sketches (Ailon & Chazelle, 2006; Ailon & Liberty, 2009), does not own the provable LSH property. Thus, it is not a desirable alternative to E2LSH because there are substantial empirical evidence that using these (non-LSH) sketches for indexing leads to a drastic bias in the expected behavior, leading to poor accuracy (Shrivastava, 2017).

Our Contribution: We develop a simple yet efficient LSH scheme (FastLSH) under l_2 norm. FastLSH involves two basic operations - random sampling and random projection, and offers (empirically) near constant time complexity instead of $O(nk)$ of E2LSH. Also, we derive the expression of the probability of collision (equity of hash values) for FastLSH and prove the asymptotic equivalence w.r.t m (the number of sampled dimensions) between FastLSH and E2LSH, which means that our proposal owns the desirable LSH property. We also rigidly analyze how m affects the probability of collision when m is relatively small. To further validate our claims, we conduct comprehensive experiments over various publicly available datasets for the ANN search task. Experimental results demonstrate that FastLSH has comparable answer accuracy and query efficiency with the classic LSH scheme, while significantly reducing the cost of hashing. Considering its simplicity and efficiency, we believe that FastLSH is a promising alternative to E2LSH in practical applications.

2. Preliminaries

In this section, we introduce notations and background knowledge used in this article. Let \mathbf{D} be the dataset of size

N in \mathbb{R}^n and $\mathbf{v} \in \mathbf{D}$ be a data point (vector) and $\mathbf{u} \in \mathbb{R}^n$ be a query vector. We denote $\phi(x) = \frac{1}{\sqrt{2\pi}} \exp(-\frac{x^2}{2})$ and $\Phi(x) = \int_{-\infty}^x \frac{1}{\sqrt{2\pi}} \exp(-\frac{x^2}{2}) dx$ as the probability density function (PDF) and cumulative distribution function (CDF) of the standard normal distribution $\mathcal{N}(0, 1)$, respectively.

2.1. Locality Sensitive Hashing

Definition 2.1. (c -Approximate R -Near Neighbor or (c, R) -NN problem) Given a set \mathbf{D} in n -dimensional Euclidean space \mathbb{R}^n and parameters $R > 0$, $\delta > 0$, construct a data structure which, for any given query point \mathbf{u} , does the following with probability $1 - \delta$: if there exists an R -near neighbor of \mathbf{u} in \mathbf{D} , it reports some cR -near neighbor of \mathbf{u} in \mathbf{D} .

Formally, an R -near neighbor of \mathbf{u} is a point \mathbf{v} such that $\|\mathbf{v} - \mathbf{u}\|_2 \leq R$. Locality Sensitive Hashing is an effectively randomized technique to solve the (c, R) -NN problem. It is a family of hash functions that can hash points into buckets, where similar points have higher probability to end up in the same bucket than dissimilar points. Consider a family \mathcal{H} of hash functions mapping \mathbb{R}^n to some universe U .

Definition 2.2. (Locality Sensitive Hashing) A hash function family $\mathcal{H} = \{h : \mathbb{R}^n \rightarrow U\}$ is called (R, cR, p_1, p_2) -sensitive if for any $\mathbf{v}, \mathbf{u} \in \mathbb{R}^n$

- if $\|\mathbf{v} - \mathbf{u}\|_2 \leq R$ then $Pr_{\mathcal{H}}[h(\mathbf{v}) = h(\mathbf{u})] \geq p_1$;
- if $\|\mathbf{v} - \mathbf{u}\|_2 \geq cR$ then $Pr_{\mathcal{H}}[h(\mathbf{v}) = h(\mathbf{u})] \leq p_2$;

In order for the LSH family to be useful, it has to satisfy $c > 1$ and $p_1 > p_2$. Please note that only hashing schemes with such a property are qualified locality sensitive hashing and can enjoy the theoretical guarantee of LSH.

2.2. LSH for l_2 Norm

(Datar et al., 2004) presents an LSH family that can be employed for l_p ($p \in (0, 2]$) norms based on p -stable distribution. When $p = 2$, it yields the well-known LSH family for l_2 norm (E2LSH). The hash function is defined as follows:

$$h_{\mathbf{a},b}(\mathbf{v}) = \left\lfloor \frac{\mathbf{a}^T \mathbf{v} + b}{w} \right\rfloor \quad (1)$$

where $\lfloor \cdot \rfloor$ is the floor operation, \mathbf{a} is a n -dimensional vector with each entry chosen independently from $\mathcal{N}(0, 1)$ and b is a real number chosen uniformly from the range $[0, w]$. w is an important parameter by which one could tune the performance of E2LSH.

For E2LSH, the probability of collision for any pair (\mathbf{v}, \mathbf{u})

under $h_{a,b}(\cdot)$ can be computed as:

$$p(s) = Pr[h_{a,b}(\mathbf{v}) = h_{a,b}(\mathbf{u})] = \int_0^w f_{|sX|}(t) \left(1 - \frac{t}{w}\right) dt \quad (2)$$

where $s = \|\mathbf{v} - \mathbf{u}\|_2$ is the Euclidean distance between (\mathbf{v}, \mathbf{u}) , and $f_{|sX|}(t)$ is the PDF of the absolute value of normal distribution sX (X is a random variable following the standard normal distribution). Given w , $p(s)$ is a monotonically decreasing function of s , which means $h_{a,b}(\cdot)$ satisfies the LSH property.

Fact 2.3. (Datar et al., 2004) Given the LSH family, a data structure can be built to solve the (c, R) -NN problem with $O(N^\rho \log N)$ query time and $O(N^{1+\rho})$ space, where $\rho = \frac{\log(1/p_1)}{\log(1/p_2)}$.

2.3. Truncated Normal Distribution

The truncated normal distribution is suggested if one need to use the normal distribution to describe the random variation of a quantity that, for physical reasons, must be strictly in the range of a truncated interval instead of $(-\infty, +\infty)$ (Cohen, 1991). The truncated normal distribution is the probability distribution derived from that of normal random variables by bounding the values from either below or above (or both). Assume that the interval (a_1, a_2) is the truncated interval, then the probability density function can be written as:

$$\psi(x; \mu, \sigma^2, a_1, a_2) = \begin{cases} 0 & x \leq a_1 \\ \frac{\phi(x; \mu, \sigma^2)}{\Phi(a_2; \mu, \sigma^2) - \Phi(a_1; \mu, \sigma^2)} & a_1 < x < a_2 \\ 0 & a_2 \leq x \end{cases} \quad (3)$$

The cumulative distribution function is:

$$\Psi(x; \mu, \sigma^2, a_1, a_2) = \begin{cases} 0 & x \leq a_1 \\ \frac{\Phi(x; \mu, \sigma^2) - \Phi(a_1; \mu, \sigma^2)}{\Phi(a_2; \mu, \sigma^2) - \Phi(a_1; \mu, \sigma^2)} & a_1 < x < a_2 \\ 1 & a_2 \leq x \end{cases} \quad (4)$$

3. Fast LSH via Random Sampling

3.1. The Proposed LSH Function Family

The cost of hashing defined in Eqn. (1) is dominated by the inner product $\mathbf{a}^T \mathbf{v}$, which takes $O(n)$ multiplication and addition operations. As mentioned in Section 1, hashing is one of the main computational bottleneck in almost all LSH applications when the number of hashes is large and the amount of data keeps increasing. To address this issue, we propose a novel family of locality sensitive hashing termed as FastLSH. Computing hash values with FastLSH involves two steps, i.e., random sampling and random projection.

In the first step, we do random sampling from n dimensions. Particularly, we draw m *i.i.d.* samples in the

range of 1 to n uniformly to form a multiset S . For every $\mathbf{v} = \{v_1, v_2, \dots, v_n\}$, we concatenate all v_i to form a m -dimensional vector $\tilde{\mathbf{v}} = \{\tilde{v}_1, \tilde{v}_2, \dots, \tilde{v}_m\}$ if $i \in S$. As a quick example, suppose $\mathbf{v} = \{1, 3, 5, 7, 9\}$ is a 5-dimensional vector and $S = \{2, 4, 2\}$. Then we can get a 3-dimensional vector $\tilde{\mathbf{v}} = \{3, 7, 3\}$ under S . It is easy to see that each entry in \mathbf{v} has equal probability $\frac{m}{n}$ of being chosen. Next, we slightly overuse notation S and denote by $S(\cdot)$ the random sampling operator. Thus, $\tilde{\mathbf{v}} \in \mathbb{R}^m = S(\mathbf{v})$ for $\mathbf{v} \in \mathbb{R}^n$ ($m < n$).

In the second step, the hash value is computed in the same way as Eqn. (1) using $\tilde{\mathbf{v}}$ instead of \mathbf{v} , and then the overall hash function is formally defined as follows:

$$h_{\tilde{\mathbf{a}}, \tilde{b}}(\mathbf{v}) = \left\lfloor \frac{\tilde{\mathbf{a}}^T S(\mathbf{v}) + \tilde{b}}{\tilde{w}} \right\rfloor \quad (5)$$

where $\tilde{\mathbf{a}} \in \mathbb{R}^m$ is the random projection vector of which each entry is chosen independently from $\mathcal{N}(0, 1)$, \tilde{w} is a user-specified constant and \tilde{b} is a real number uniformly drawn from $[0, \tilde{w}]$. The hash function $h_{\tilde{\mathbf{a}}, \tilde{b}}(\mathbf{v})$ maps a n -dimensional vector \mathbf{v} onto the set of integers.

Compared with E2LSH, FastLSH reduces the cost of hashing from $O(n)$ to $O(m)$. As will be discussed in Section 6, a relatively small $m < n$ suffices to provide competitive performance against E2LSH, which leads to significant performance gain in hash function evaluation.

3.2. ANN Search Using FastLSH

FastLSH can be easily plugged into any existing LSH applications considering its simplicity. This section gives a brief discussion about how to use FastLSH for ANN search.

The canonical LSH index structure for ANN search is built as follows. A hash code $H(\mathbf{v}) = (h_1(\mathbf{v}), h_2(\mathbf{v}), \dots, h_k(\mathbf{v}))$ is computed using k independent LSH functions (i.e., $H(\mathbf{v})$ is the concatenation of k elementary LSH codes). Then a hash table is constructed by adding the 2-tuple $\langle H(\mathbf{v}), id \text{ of } \mathbf{v} \rangle$ into corresponding bucket. To boost accuracy, L groups of hash functions $H_i(\cdot), i = 1, \dots, L$ are drawn independently and uniformly at random from the LSH family, resulting in L hash tables. To use FastLSH in such a ANN search framework, the only modification is to replace hash function definitin in Eqn. (1) with that of Eqn. (5).

To answer a query \mathbf{u} , one need to first compute $H_1(\mathbf{u}), \dots, H_L(\mathbf{u})$ and then search all these L buckets to obtain the combined set of candidates. There exists two ways (approximate and exact) to process these candidates. In the approximate version, we only evaluate no more than $3L$ points in the candidate set. The LSH theory ensures that the (c, R) -NN is found with a constant probability. In practice, however, the exact one is widely used since it offers

better accuracy at the cost of evaluating all points in the candidate set (Datar et al., 2004). The search time consists of both the hashing time and the time taken to prune the candidate set for the exact version. In this paper, we use the exact method to process a query similar to (Datar et al., 2004; Andoni, 2005).

4. Theoretical Analysis

While FastLSH is easy to comprehend and simple to implement, it is non-trivial to show that the proposed LSH function meets the LSH property, i.e., the probability of collision for (\mathbf{v}, \mathbf{u}) decreases with their l_2 norm increasing. In this section, we will first derive the probability of collision for FastLSH, and prove that its asymptotic behavior is equivalent to E2LSH. Then, by using both rigid analysis and the numerical method, we demonstrate that FastLSH still owns desirable LSH property when m is relatively small.

4.1. Probability of Collision

For given vector pair (\mathbf{v}, \mathbf{u}) , let $s = \|\mathbf{v} - \mathbf{u}\|_2$. For our purpose, the collection of n entries $(v_i - u_i)^2 \{i = 1, 2, \dots, n\}$ is viewed as a population, which follows an unknown distribution with finite mean $\mu = (\sum_{i=1}^n (v_i - u_i)^2)/n$ and variance $\sigma^2 = (\sum_{i=1}^n ((v_i - u_i)^2 - \mu)^2)/n$. After performing the sampling operator $S(\cdot)$ of size m , \mathbf{v} and \mathbf{u} are transformed into $\tilde{\mathbf{v}} = S(\mathbf{v})$ and $\tilde{\mathbf{u}} = S(\mathbf{u})$, and the squared distance of $(\tilde{\mathbf{v}}, \tilde{\mathbf{u}})$ is $\tilde{s}^2 = \sum_{i=1}^m (\tilde{v}_i - \tilde{u}_i)^2$. By Central Limit Theorem, we have the following lemma:

Lemma 4.1. *If m is sufficiently large, then the sum \tilde{s}^2 of m i.i.d. random samples $(\tilde{v}_i - \tilde{u}_i)^2$ ($i \in 1, 2, \dots, m$) converges asymptotically to the normal distribution with mean $m\mu$ and variance $m\sigma^2$, i.e., $\tilde{s}^2 \sim \mathcal{N}(m\mu, m\sigma^2)$.*

Lemma 4.1 states that the squared distance between $\tilde{\mathbf{v}}$ and $\tilde{\mathbf{u}}$ follows a normal distribution for large m . Practically, a small m (say 30) often suffices to make the sampling distribution of the sample mean approaches the normal in real-life applications (Islam, 2018; Feller, 1991).

Random variable \tilde{s}^2 , however, does not follow exactly the normal distribution since $\tilde{s}^2 \geq 0$ whereas the range of definition of the normal distribution is $(-\infty, +\infty)$. A mathematically defensible way to preserve the main features of the normal distribution while avoiding negative values involves *the truncated normal distribution*, in which the range of definition is made finite at one or both ends of the interval.

Particularly, \tilde{s}^2 can be modeled by normal distribution $\tilde{s}^2 \sim \mathcal{N}(m\mu, m\sigma^2)$ over the truncation interval $[0, +\infty)$, that is, the singly-truncated normal distribution $\psi(x; \tilde{\mu}, \tilde{\sigma}^2, 0, +\infty)$. Considering the fact that $\tilde{s} \geq 0$, we have $Pr[\tilde{s} < t] = Pr[\tilde{s}^2 < t^2]$ for any $t > 0$. Therefore, the CDF of \tilde{s} ,

denoted by $F_{\tilde{s}}$, can be computed as follows:

$$\begin{aligned} F_{\tilde{s}}(t) &= Pr[\tilde{s} < t] = Pr[\tilde{s}^2 < t^2] \\ &= \int_0^{t^2} \psi(x; \tilde{\mu}, \tilde{\sigma}^2, 0, \infty) dx \end{aligned} \quad (6)$$

where $\tilde{\mu} = m\mu$ and $\tilde{\sigma}^2 = m\sigma^2$. Due to the fact that the PDF is the derivative of the CDF, the PDF of \tilde{s} , denoted by $f_{\tilde{s}}$, is derived as follows:

$$f_{\tilde{s}}(t) = \frac{d}{dt}[F_{\tilde{s}}(t)] = 2t\psi(t^2; \tilde{\mu}, \tilde{\sigma}^2, 0, \infty) \quad (7)$$

Recall that \mathbf{a} is a projection vector with entries being *i.i.d* samples drawn from $\mathcal{N}(0, 1)$. It follows from the p -stability that the distance between projections $(\mathbf{a}^T \mathbf{v} - \mathbf{a}^T \mathbf{u})$ for two vectors \mathbf{v} and \mathbf{u} is distributed as $\|\mathbf{v} - \mathbf{u}\|_2 X$, i.e., sX , where $X \sim \mathcal{N}(0, 1)$ (Zolotarev, 1986; Datar et al., 2004). Similarly, the projection distance between $\tilde{\mathbf{v}}$ and $\tilde{\mathbf{u}}$ under $\tilde{\mathbf{a}}$ ($\tilde{\mathbf{a}}^T \tilde{\mathbf{v}} - \tilde{\mathbf{a}}^T \tilde{\mathbf{u}}$) follows the distribution $\tilde{s}X$. Note that the PDF of sX , i.e., $f_{sX}(x) = \frac{1}{s}\phi(\frac{x}{s})$, is an important factor in calculating the probability of collision in Eqn. (2). Hence, we need to get the PDF of $\tilde{s}X$ first in order to derive the probability of collision for FastLSH.

Although we know the distributions of both \tilde{s} and X , it is not straight-forward to figure out the distribution of their product $\tilde{s}X$. Fortunately, Lemma 4.2 gives the characteristic function of random variable $W = XY$, where X and Y are two independent random variables, one following a standard normal distribution and the other following a distribution with mean μ and variance σ^2 .

Lemma 4.2. *The characteristic function of the product of two independent random variables $W = XY$ is as follows:*

$$\varphi_W(x) = E_Y\{\exp(-\frac{x^2 Y^2}{2})\}$$

where X is a standard normal random variable and Y is an independent random variable with mean μ and variance σ^2 .

Proof. See Appendix A.1 □

Note that the distribution of a random variable is determined uniquely by its characteristic function. With respect to $\tilde{s}X$, the characteristic function can be obtained by Lemma 4.2 since X follows the standard normal:

Lemma 4.3. *The characteristic function of $\tilde{s}X$ is as follows:*

$$\begin{aligned} \varphi_{\tilde{s}X}(x) &= \frac{1}{2(1 - \Phi(\frac{-\tilde{\mu}}{\tilde{\sigma}}))} \exp(\frac{1}{8}x^4\tilde{\sigma}^2 - \frac{1}{2}\tilde{\mu}x^2) \\ &\cdot \operatorname{erfc}(\frac{\frac{1}{2}x^2\tilde{\sigma}^2 - \tilde{\mu}}{\sqrt{2}\tilde{\sigma}}) \quad (-\infty < x < +\infty) \end{aligned}$$

where $\operatorname{erfc}(t) = \frac{2}{\sqrt{\pi}} \int_t^{+\infty} \exp(-x^2) dx$ ($-\infty < t < +\infty$) is the complementary error function.

Proof. See Appendix A.2 \square

Given the characteristic function, the probability density function can be obtained through the inverse Fourier transformation. Thus, the PDF of $\tilde{s}X$, denoted by $f_{\tilde{s}X}(t)$, is as follows:

$$f_{\tilde{s}X}(t) = \frac{1}{2\pi} \int_{-\infty}^{+\infty} \exp(-itx) \varphi_{\tilde{s}X}(x) dx \quad (8)$$

where the symbol $i = \sqrt{-1}$ represents the imaginary unit.

Now we are in the position to derive the probability of collision for vector pair (\mathbf{v}, \mathbf{u}) under the proposed LSH function in Eqn. (5). Let $f_{|\tilde{s}X|}(t)$ represent the PDF of the absolute value of $\tilde{s}X$. It is easy to obtain the collision probability $p(s, \sigma)$ for FastLSH by replacing $f_{|\tilde{s}X|}(t)$ in Eqn. (2) with $f_{|\tilde{s}X|}(t)$.

Theorem 4.4.

$$\begin{aligned} p(s, \sigma) &= Pr[h_{\tilde{a}, \tilde{b}}(\mathbf{v}) = h_{\tilde{a}, \tilde{b}}(\mathbf{u})] \\ &= \int_0^{\tilde{w}} f_{|\tilde{s}X|}(t) \left(1 - \frac{t}{\tilde{w}}\right) dt \end{aligned} \quad (9)$$

Proof. See Appendix A.3 \square

We can see that, unlike E2LSH, the probability of collision $p(s, \sigma)$ depends on both s and σ . From this point of view, FastLSH can be regarded as a generalized version of E2LSH by considering one additional impact factor, i.e., the variation in the squared distance of each dimension for vector pair (\mathbf{v}, \mathbf{u}) , making it is more difficult to prove its LSH property. The influence of σ on $p(s, \sigma)$ will be discussed in the next section.

4.2. The LSH Property of FastLSH

In this section, we first prove that the asymptotic behavior of FastLSH is identical to E2LSH, and then demonstrate by both theoretical analysis and numerical computation that FastLSH owns the LSH property even for limited m .

Fact 4.5. (Datar et al., 2004) For E2LSH, $f_{sX}(t)$ follows the normal distribution $\mathcal{N}(0, s^2)$ and the collision probability $p(s)$ with bucket width w is equal to $p(\alpha s)$ under the bucket width αw , i.e., $p_w(s) = p_{\alpha w}(\alpha s)$ where $\alpha > 0$.

From Eqn. (2) and Eqn. (9), one can see that the expressions of the probability of collision for E2LSH and FastLSH are quite similar. Actually, if $f_{\tilde{s}X}(t)$ also follows normal distribution with zero mean, we can always scale \tilde{w} to make $p_w(s) = p_{\tilde{w}}(s, \sigma)$ based on Fact 4.5. The following theorem gives the asymptotic behavior of the characteristic function of $\tilde{s}X$.

Theorem 4.6.

$$\lim_{m \rightarrow +\infty} \frac{\varphi_{\tilde{s}X}(x)}{\exp\left(-\frac{ms^2x^2}{2n}\right)} = 1$$

where $|x| \leq O(m^{-1/2})$ and $\exp\left(-\frac{ms^2x^2}{2n}\right)$ is the characteristic function of $\mathcal{N}\left(0, \frac{ms^2}{n}\right)$.

Proof. See Appendix A.4. \square

Note that $\exp\left(-\frac{ms^2x^2}{2n}\right)$, the characteristic function of $\mathcal{N}\left(0, \frac{ms^2}{n}\right)$, is a bell-shaped function like the PDF of normal distributions. As a result, Theorem 4.6 implies that $\varphi_{\tilde{s}X}(x)$ is asymptotically identical to $\exp\left(-\frac{ms^2x^2}{2n}\right)$ within interval $[-\mathcal{K}\sqrt{\frac{n}{ms^2}}, +\mathcal{K}\sqrt{\frac{n}{ms^2}}]$, that is, $2\mathcal{K}$ ‘‘standard deviations’’, where \mathcal{K} is an arbitrarily large constant. Because a probability distribution is uniquely determined by its characteristic function and both $\varphi_{\tilde{s}X}(x)$ and $\exp\left(-\frac{ms^2x^2}{2n}\right)$ approach 0 when x tends to infinity, we immediately have the following Corollary.

Corollary 4.7. $f_{\tilde{s}X}(t) \sim$ the PDF of $\mathcal{N}\left(0, \frac{ms^2}{n}\right)$ as m approaches infinity.

By Corollary 4.7, $p(s) = p(s, \sigma)$ asymptotically if $\tilde{w} = \frac{m}{n}w$, meaning that σ has no effect on the probability of collision. In practical scenarios, m is often limited. Next, we study the relation between $f_{\tilde{s}X}(t)$ and the PDF of $\mathcal{N}\left(0, \frac{ms^2}{n}\right)$ when m is relatively small ($m < n$). Particularly, we derive the first four moments of $\tilde{s}X$ and $\mathcal{N}\left(0, \frac{ms^2}{n}\right)$, and analyze how m and σ affect their similarity. While in general the first four moments, or even the whole moment sequence may not determine a distribution (Lin, 2017), practitioners find that distributions near the normal can be decided very well given the first four moments (Leslie, 1959; Johnson, 1949; Ramberg et al., 1979).

Lemma 4.8.

$$\begin{cases} E(\tilde{s}X) = 0 \\ E((\tilde{s}X)^2) = \frac{ms^2}{n}(1 + \epsilon) \\ E((\tilde{s}X)^3) = 0 \\ E((\tilde{s}X)^4) = \frac{3m^2s^4}{n^2}(1 + \lambda) \end{cases}$$

where $\epsilon = \frac{\tilde{\sigma} \exp\left(\frac{-\tilde{\mu}^2}{2\tilde{s}^2}\right)}{\sqrt{2\pi}\tilde{\mu}(1 - \Phi\left(\frac{-\tilde{\mu}}{\tilde{\sigma}}\right))}$ and $\lambda = \frac{\tilde{\sigma}^2}{\tilde{\mu}^2} + \epsilon$.

Proof. See Appendix A.5 \square

Fact 4.9. (Hoel et al., 1971) The first four moments of $\mathcal{N}\left(0, \frac{ms^2}{n}\right)$ are:

$$\begin{cases} E(sX) = 0 \\ E((sX)^2) = \frac{ms^2}{n} \\ E((sX)^3) = 0 \\ E((sX)^4) = \frac{3m^2s^4}{n^2} \end{cases}$$

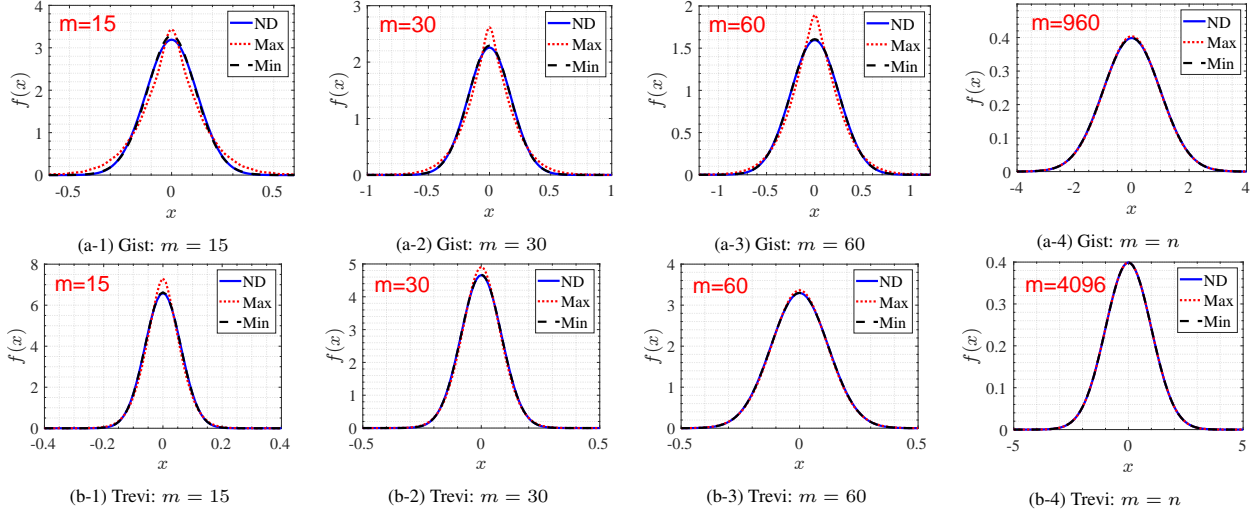


Figure 1. Comparison of probability density curves of $\mathcal{N}(0, \frac{ms^2}{n})$ (ND) and $\tilde{s}X$ under different m over datasets *Gist* and *Trevis*.

It is easy to see that ϵ and λ are monotonously decreasing function of m and increasing function of σ ($\frac{\sigma}{u} = \frac{\sigma n}{\sqrt{ms^2}}$). Hence, the first four moments of sX and $\tilde{s}X$ are equal with each other, respectively, as m approaches infinity. This is consistent with Corollary 4.7.

For limited $m < n$, the impact of σ is not negligible. However, we can easily adjust m to control the impact of σ (the data-dependent factor) on $f_{\tilde{s}X}(t)$ within a reasonable range. Table 2 in Appendix C lists the values of ϵ and λ for different m over 12 datasets, where ϵ and λ are calculated using the maximum, mean and minimum σ , respectively. As expected, ϵ and λ decrease as m increases. Take *Trevis* as an example, ϵ is equal to 0 and λ is very tiny (0.0001-0.000729) when $m = n$, manifesting the equivalence between $f_{\tilde{s}X}(t)$ and the PDF of $\mathcal{N}(0, \frac{ms^2}{n})$ as depicted in Figure 1 (b-4). In the case of $m = 30$, it also suffices to provide small enough ϵ and λ , indicating the high similarity between the distribution of $\tilde{s}X$ and $\mathcal{N}(0, \frac{ms^2}{n})$.

To visualize the similarity, we plot $f_{\tilde{s}X}(t)$ for different m under the maximum and minimum σ , and the PDF of $\mathcal{N}(0, \frac{ms^2}{n})$ in Figure 1 for two datasets *Gist* and *Trevis*. More plots for other datasets are listed in Figure 4 in Appendix C. Three observations can be made from these figures: (1) the distribution of $\tilde{s}X$ matches very well with $\mathcal{N}(0, \frac{ms^2}{n})$ for small σ ; (2) for large σ , $f_{\tilde{s}X}(t)$ differs only slightly from the PDF of $\mathcal{N}(0, \frac{ms^2}{n})$ for all m , indicating that s is the dominating factor in $p(s, \sigma)$; (3) greater m results in higher similarity between $f_{\tilde{s}X}(t)$ and $\mathcal{N}(0, \frac{ms^2}{n})$, implying that FastLSH can always achieve almost the same performance as E2LSH by choosing m appropriately.

To further validate the LSH property of FastLSH, we compare the important parameter ρ for FastLSH and E2LSH

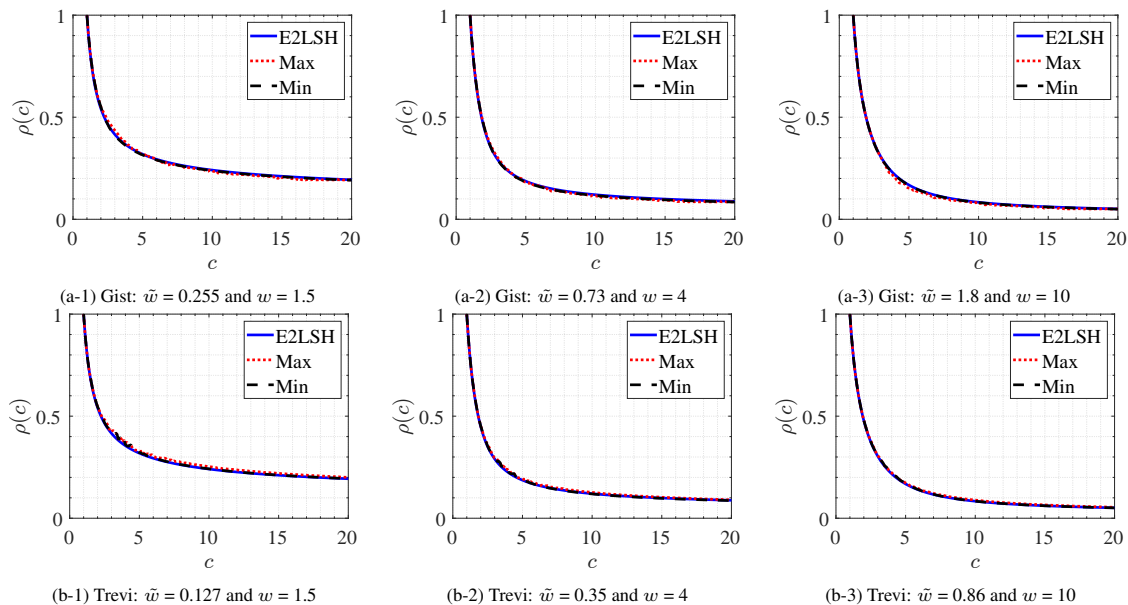
when $m = 30$. ρ is defined as the function of the approximation ratio c , i.e., $\rho(c) = \log(1/p(s_1))/\log(1/p(s_2))$, where $s_1 = 1$ and $s_2 = c$. Note that ρ affects both the space and time efficiency of LSH algorithms. For c in the range $[1, 20]$ (with increments of 0.1), we calculate ρ using *Matlab*, where the minimal and maximal σ are collected for different c (s). The plots of $\rho(c)$ under different bucket widths over the datasets *Gist* and *Trevis* are illustrated in Figure 2. Clearly, the $\rho(c)$ curve of FastLSH matches very well with that of E2LSH, verifying that FastLSH maintains almost the same LSH property with E2LSH even when m is relatively small. More plots of $\rho(c)$ for other datasets are given in Figure 5 and Figure 6 in Appendix C.

5. Extension to Other Similarity Metrics

In this section, we sketch how to extend FastLSH to other similarity measures. Since the angular similarity can be well approximated by the Euclidean distance if the norms of data item are identical, one can use FastLSH for the angular similarity directly after data normalization. In addition, FastLSH can solve the maximum inner product search problem by utilizing two transformation functions (Bachrach et al., 2014). The detailed discussion is given in Appendix B. The extension of FastLSH to support l_p norm for $p \in (0, 2)$ is left as our future work.

6. Experiments

In this section we evaluate the performance of FastLSH against other LSH algorithms for the ANN search task. All algorithms follow the standard hash table construction and search procedure as discussed in Section 3.2. All experiments are carried out on the server with six-cores Intel(R),

Figure 2. ρ curves under different bucket widths over datasets *Gist* and *Trevi*

i7-8750H @ 2.20GHz CPUs and 32 GB RAM, in Ubuntu 20.04.

Datasets: 11 publicly available high-dimensional real datasets and one synthetic dataset are experimented with (Li et al., 2019), the statistics of which are listed in Table 1. Sun¹ is the set of containing about 70k GIST features of images. Cifar² is denoted as the set of 50k vectors extracted from TinyImage. Audio³ is the set of about 50k vectors extracted from DARPA TIMIT. Trevi⁴ is the set of containing around 100k features of bitmap images. Notre⁵ is the set of features that are Flickr images and a reconstruction. Sift⁶ is the set of containing 1 million SIFT vectors. Gist⁷ is the set that is consist of 1 million image vectors. Deep⁸ is the set of 1 million vectors that are deep neural codes of natural images obtained by convolutional neural network. Ukbench⁹ is the set of vectors containing 1 million features of images. Glove¹⁰ is the set of about 1.2 million feature vectors extracted from Tweets. ImageNet¹¹ is the set of data points containing about 2.4 million dense SIFT features. Random is the set containing 1 million randomly selected vectors in a unit hypersphere.

¹<http://groups.csail.mit.edu/vision/SUN/>

²<http://www.cs.toronto.edu/~kriz/cifar.html>

³<http://www.cs.princeton.edu/cass/audio.tar.gz>

⁴<http://phototour.cs.washington.edu/patches/default.htm>

⁵<http://phototour.cs.washington.edu/datasets/>

⁶<http://corpus-texmex.irisa.fr>

⁷<https://github.com/aaalgo/kgraph>

⁸https://yadi.sk/d/I_yaFVqchJmoc

⁹<http://vis.uky.edu/~stewe/ukbench/>

¹⁰<http://nlp.stanford.edu/projects/glove/>

¹¹<http://cloudev.org/objdetect/>

Table 1. Statistics of Datasets

Datasets	# of Points	# of Queries	Dimension
Sun	69106	200	512
Cifar	50000	200	512
Audio	53387	200	192
Trevi	99000	200	4096
Notre	333000	200	128
Sift	1000000	200	128
Gist	1000000	200	960
Deep	1000000	200	256
Ukbench	1000000	200	128
Glove	1192514	200	100
ImageNet	2340000	200	150
Random	1000000	200	100

Baselines: We compare FastLSH with two popular LSH algorithms, i.e., E2LSH (Datar et al., 2004; Andoni, 2005) and ACHash (Dasgupta et al., 2011). E2LSH is the vanilla LSH scheme for approximate near neighbor search with sub-linear query time. ACHash is proposed to speedup the hash function evaluation by using Hadamard transform and sparse random projection. Note that ACHash is actually not an eligible LSH method because no expression of the probability of collision exists for ACHash, not mentioning the desirable LSH property. We choose ACHash as one of the baselines for the sake of completeness.

Evaluation Metrics: To evaluate the performance of FastLSH and baselines, we present the following metrics: 1) the average recall, i.e., the fraction of near neighbors that are actually returned; 2) the average running time to report the near neighbors for each query; 3) the time taken to compute hash functions.

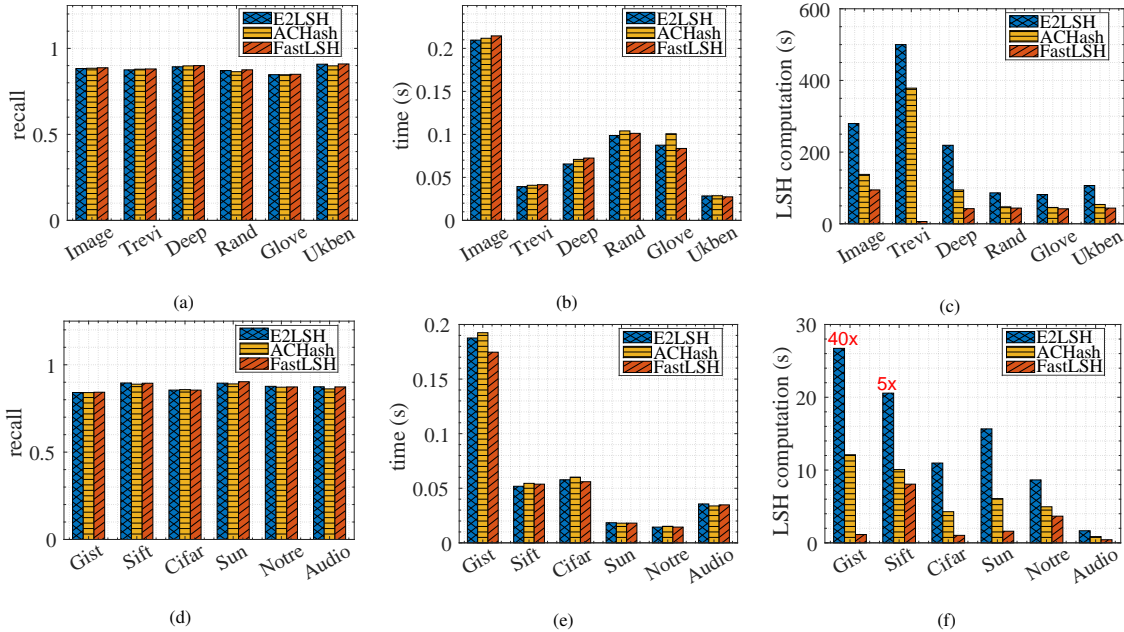


Figure 3. Comparison of recall, average query time and LSH computation time.

Parameter Settings: For the same dataset and target recall, we use identical k (number of hash functions per table) and L (number of hash tables) for fairness. Thus, three algorithms take the same space occupations. m is set to 30 throughout all experiments for FastLSH. To achieve optimal performance, the sampling ratio for ACHash is set to the default 0.25. We report R10@10 over all of the datasets for three algorithms.

Experiment 1: In this set of experiments, we set the target recall as 0.9. By tuning L , k and bucket widths, the three methods achieve almost the same recall on the same dataset with the optimal query time¹². The recall, average query time and LSH computation time are illustrated in Figure 3 (a), (b), (d) and (e). As analyzed in Section 4.2, FastLSH and E2LSH owns similar theoretical property, and thus achieve comparable query performance and answer accuracy as plotted in Figure 3. Due to lack of theoretical guarantee, ACHash performs slightly worse than FastLSH and E2LSH in most cases w.r.t query efficiency.

The performance of the three methods differs dramatically when it turns to the cost of hashing. As shown in Figure 3 (c) and (f), the LSH computation time of FastLSH is significantly superior to E2LSH and ACHash. For example, FastLSH obtains around 80 speedup over E2LSH and runs 60 times faster than ACHash on *Trevi*. This is because the time complexity of FastLSH is only $O(m)$ instead of $O(n)$ of E2LSH. For ACHash, the fixed sampling ratio and overhead in Hadamard transform make it inferior to FastLSH.

¹²The actual recall may vary around 0.9 slightly

Experiment 2: We also plot the recall v.s. average query time curves by varying target recalls to obtain a complete picture of FastLSH, which are depicted in Figure 7 in Appendix C due to space limitation. The empirical results demonstrate that FastLSH performs almost the same in terms of answer accuracy, query efficiency and space occupation as E2LSH. This further validates that FastLSH owns the same LSH property as E2LSH with limited $m < n$. Again, ACHash is slightly inferior to the others in most cases.

In sum, FastLSH is on par with E2LSH (with provable LSH property) in terms of answer accuracy and query efficiency and marginally superior to ACHash (without provable LSH property), while significantly reducing the cost of hashing. We believe that FastLSH is a promising alternative to the existing hashing schemes for l_2 norm.

7. Conclusion

In this paper, we develop FastLSH to accelerate hash function evaluation, which maintains the same theoretical guarantee and empirical performance as the classic E2LSH. Rigid analysis shows that the probability of collision of FastLSH is asymptotically equal to that of E2LSH. In the case of limited m , we quantitatively analyze the impact of σ and m on the probability of collision. Extensive experiments on a number of datasets demonstrate that FastLSH is a promising alternative to the classic LSH scheme.

References

- Ailon, N. and Chazelle, B. Approximate nearest neighbors and the fast johnson-lindenstrauss transform. In *Proceedings of the thirty-eighth annual ACM symposium on Theory of computing*, pp. 557–563, 2006.
- Ailon, N. and Liberty, E. Fast dimension reduction using rademacher series on dual bch codes. *Discrete & Computational Geometry*, 42:615–630, 2009.
- Andoni, A. E2lsh-0.1 user manual. <http://web.mit.edu/andoni/www/LSH/index.html>, 2005.
- Andoni, A. and Indyk, P. Near-optimal hashing algorithms for approximate nearest neighbor in high dimensions. *Communications of the ACM*, 51(1):117–122, 2008.
- Bachrach, Y., Finkelstein, Y., Gilad-Bachrach, R., Katzir, L., Koenigstein, N., Nice, N., and Paquet, U. Speeding up the xbox recommender system using a euclidean transformation for inner-product spaces. In *Proceedings of the 8th ACM Conference on Recommender systems*, pp. 257–264, 2014.
- Bentley, J. L. Multidimensional binary search trees used for associative searching. *Communications of the ACM*, 18(9):509–517, 1975.
- Charikar, M. S. Similarity estimation techniques from rounding algorithms. In *Proceedings of the thirty-fourth annual ACM symposium on Theory of computing*, pp. 380–388, 2002.
- Chen, B., Medini, T., Farwell, J., Tai, C., Shrivastava, A., et al. Slide: In defense of smart algorithms over hardware acceleration for large-scale deep learning systems. *Proceedings of Machine Learning and Systems*, 2:291–306, 2020.
- Chen, C., Horng, S.-J., and Huang, C.-P. Locality sensitive hashing for sampling-based algorithms in association rule mining. *Expert Systems with Applications*, 38(10):12388–12397, 2011.
- Cohen, A. C. *Truncated and censored samples: theory and applications*. CRC press, 1991.
- Dasgupta, A., Kumar, R., and Sarlós, T. Fast locality-sensitive hashing. In *Proceedings of the 17th ACM SIGKDD international conference on Knowledge discovery and data mining*, pp. 1073–1081, 2011.
- Datar, M., Immorlica, N., Indyk, P., and Mirrokni, V. S. Locality-sensitive hashing scheme based on p-stable distributions. In *Proceedings of the twentieth annual symposium on Computational geometry*, pp. 253–262, 2004.
- Feller, W. *An introduction to probability theory and its applications, Volume 2*, volume 81. John Wiley & Sons, 1991.
- Gan, J., Feng, J., Fang, Q., and Ng, W. Locality-sensitive hashing scheme based on dynamic collision counting. In *Proceedings of the 2012 ACM SIGMOD international conference on management of data*, pp. 541–552, 2012.
- Hoel, P. G., Port, S. C., and Stone, C. J. *Introduction to probability theory*. Houghton Mifflin, 1971.
- Huang, Q., Feng, J., Zhang, Y., Fang, Q., and Ng, W. Query-aware locality-sensitive hashing for approximate nearest neighbor search. *Proceedings of the VLDB Endowment*, 9(1):1–12, 2015.
- Indyk, P. and Motwani, R. Approximate nearest neighbors: towards removing the curse of dimensionality. In *Proceedings of the thirtieth annual ACM symposium on Theory of computing*, pp. 604–613, 1998.
- Islam, M. R. Sample size and its role in central limit theorem (clt). *International Journal of Physics and Mathematics*, 1(1):37–47, 7 2018.
- Johnson, N. L. Systems of frequency curves generated by methods of translation. *Biometrika*, 36(1/2):149–176, 1949.
- Katayama, N. and Satoh, S. The sr-tree: An index structure for high-dimensional nearest neighbor queries. *ACM Sigmod Record*, 26(2):369–380, 1997.
- Koga, H., Ishibashi, T., and Watanabe, T. Fast agglomerative hierarchical clustering algorithm using locality-sensitive hashing. *Knowledge and Information Systems*, 12:25–53, 2007.
- Kushilevitz, E., Ostrovsky, R., and Rabani, Y. Efficient search for approximate nearest neighbor in high dimensional spaces. In *Proceedings of the thirtieth annual ACM symposium on Theory of computing*, pp. 614–623, 1998.
- Leslie, D. Determination of parameters in the johnson system of probability distributions. *Biometrika*, 46(1/2): 229–231, 1959.
- Li, W., Zhang, Y., Sun, Y., Wang, W., Li, M., Zhang, W., and Lin, X. Approximate nearest neighbor search on high dimensional data—experiments, analyses, and improvement. *IEEE Transactions on Knowledge and Data Engineering*, 32(8):1475–1488, 2019.
- Lin, G. D. Recent developments on the moment problem. *Journal of Statistical Distributions and Applications*, 4(1):5, 2017.

- Lu, K. and Kudo, M. R2lsh: A nearest neighbor search scheme based on two-dimensional projected spaces. In *2020 IEEE 36th International Conference on Data Engineering (ICDE)*, pp. 1045–1056. IEEE, 2020.
- Lv, Q., Josephson, W., Wang, Z., Charikar, M., and Li, K. Multi-probe lsh: efficient indexing for high-dimensional similarity search. In *Proceedings of the 33rd international conference on Very large data bases*, pp. 950–961, 2007.
- Ramberg, J. S., Dudewicz, E. J., Tadikamalla, P. R., and Mykytka, E. F. A probability distribution and its uses in fitting data. *Technometrics*, 21(2):201–214, 1979.
- Samet, H. *Foundations of multidimensional and metric data structures*. Morgan Kaufmann, 2006.
- Shrivastava, A. Optimal densification for fast and accurate minwise hashing. In *International Conference on Machine Learning*, pp. 3154–3163. PMLR, 2017.
- Shrivastava, A. and Li, P. Asymmetric lsh (alsh) for sublinear time maximum inner product search (mips). *Advances in neural information processing systems*, 27:2321–2329, 2014a.
- Shrivastava, A. and Li, P. Densifying one permutation hashing via rotation for fast near neighbor search. In *International Conference on Machine Learning*, pp. 557–565. PMLR, 2014b.
- Sun, Y., Wang, W., Qin, J., Zhang, Y., and Lin, X. Srs: solving c-approximate nearest neighbor queries in high dimensional euclidean space with a tiny index. *Proceedings of the VLDB Endowment*, 2014.
- Sundaram, N., Turmukhametova, A., Satish, N., Mostak, T., Indyk, P., Madden, S., and Dubey, P. Streaming similarity search over one billion tweets using parallel locality-sensitive hashing. *Proceedings of the VLDB Endowment*, 6(14):1930–1941, 2013.
- Tao, Y., Yi, K., Sheng, C., and Kalnis, P. Efficient and accurate nearest neighbor and closest pair search in high-dimensional space. *ACM Transactions on Database Systems (TODS)*, 35(3):1–46, 2010.
- Tian, Y., Zhao, X., and Zhou, X. Db-lsh: Locality-sensitive hashing with query-based dynamic bucketing. In *2022 IEEE 38th International Conference on Data Engineering (ICDE)*, pp. 2250–2262. IEEE, 2022.
- Yang, C., Deng, D., Shang, S., and Shao, L. Efficient locality-sensitive hashing over high-dimensional data streams. In *2020 IEEE 36th International Conference on Data Engineering (ICDE)*, pp. 1986–1989. IEEE, 2020.
- Zheng, B., Xi, Z., Weng, L., Hung, N. Q. V., Liu, H., and Jensen, C. S. Pm-lsh: A fast and accurate lsh framework for high-dimensional approximate nn search. *Proceedings of the VLDB Endowment*, 13(5):643–655, 2020.
- Zolotarev, V. M. *One-dimensional stable distributions*, volume 65 of *Translations of Mathematical Monographs*. American Mathematical Society, 1986.

Appendix

A. Proofs

Lemma A.1. *The characteristic function of the product of two independent random variables $W = XY$ is as follows:*

$$\varphi_W(x) = E_Y \left\{ \exp\left(-\frac{x^2 Y^2}{2}\right) \right\}$$

where X is a standard normal random variable and Y is an independent random variable with mean μ and variance σ^2 .

Proof. For the characteristic function of W , we can write:

$$\begin{aligned} \varphi_W(x) &= E_W \{ \exp(ixW) \} \\ &= E_{XY} \{ \exp(ixXY) \} \\ &= E_Y \{ E_{X|Y} \{ \exp(ixXY) | Y \} \} \\ &= \int_{-\infty}^{+\infty} E_{X|Y} \{ \exp(-ixXY) | Y \} f(Y) dY \\ &= \int_{-\infty}^{+\infty} \left(\int_{-\infty}^{+\infty} \exp(-ixXY) f(X|Y) dX \right) f(Y) dY \\ &= \int_{-\infty}^{+\infty} \exp\left(-\frac{x^2 Y^2}{2}\right) f(Y) dY \\ &= E_Y \left\{ \exp\left(-\frac{x^2 Y^2}{2}\right) \right\} \end{aligned}$$

where standard normal random variable X is eliminated by its characteristic function. We prove this Lemma. \square

Lemma A.2. *The characteristic function of $\tilde{s}X$ is as follows:*

$$\varphi_{\tilde{s}X}(x) = \frac{1}{2(1 - \Phi(\frac{-\tilde{\mu}}{\tilde{\sigma}}))} \exp\left(\frac{1}{8}x^4\tilde{\sigma}^2 - \frac{1}{2}\tilde{\mu}x^2\right) \operatorname{erfc}\left(\frac{\frac{1}{2}x^2\tilde{\sigma}^2 - \tilde{\mu}}{\sqrt{2}\tilde{\sigma}}\right) \quad (-\infty < x < +\infty)$$

where $\operatorname{erfc}(t) = \frac{2}{\sqrt{\pi}} \int_t^{+\infty} \exp(-x^2) dx$ ($-\infty < t < +\infty$) is the complementary error function.

Proof. According to Eqn. (7), we know the PDF of $\tilde{s}X$. By applying Lemma A.1, we have the following result:

$$\begin{aligned} \varphi_{\tilde{s}X}(x) &= \frac{1}{\sqrt{2\pi\tilde{\sigma}}} \int_0^{+\infty} \frac{2y}{\Phi(a_2; \tilde{\mu}, \tilde{\sigma}^2) - \Phi(a_1; \tilde{\mu}, \tilde{\sigma}^2)} \exp\left(\frac{-x^2 y^2}{2} - \frac{(y^2 - \tilde{\mu})^2}{2\tilde{\sigma}^2}\right) dy \\ &= \frac{1}{\sqrt{2\pi\tilde{\sigma}}} \int_0^{+\infty} \frac{1}{\Phi(a_2; \tilde{\mu}, \tilde{\sigma}^2) - \Phi(a_1; \tilde{\mu}, \tilde{\sigma}^2)} \exp\left(-\frac{x^2 y^2}{2} - \frac{(y^2 - \tilde{\mu})^2}{2\tilde{\sigma}^2}\right) dy^2 \\ &= \frac{1}{\sqrt{2\pi\tilde{\sigma}}} \int_0^{+\infty} \frac{1}{\Phi(a_2; \tilde{\mu}, \tilde{\sigma}^2) - \Phi(a_1; \tilde{\mu}, \tilde{\sigma}^2)} \exp\left(\frac{-(y^2 - (\tilde{\mu} - \frac{1}{2}x^2\tilde{\sigma}^2))^2 - \tilde{\mu}x^2\tilde{\sigma}^2 + \frac{1}{4}x^4\tilde{\sigma}^4}{2\tilde{\sigma}^2}\right) dy^2 \\ &= \frac{1}{\sqrt{2\pi\tilde{\sigma}}} \int_0^{+\infty} \frac{1}{\Phi(a_2; \tilde{\mu}, \tilde{\sigma}^2) - \Phi(a_1; \tilde{\mu}, \tilde{\sigma}^2)} \exp\left(\frac{1}{8}x^4\tilde{\sigma}^2 - \frac{1}{2}\tilde{\mu}x^2\right) \exp\left(\frac{-(y^2 - (\tilde{\mu} - \frac{1}{2}x^2\tilde{\sigma}^2))^2}{2\tilde{\sigma}^2}\right) dy^2 \\ &= \frac{1}{2(\Phi(\frac{a_2 - \tilde{\mu}}{\tilde{\sigma}}) - \Phi(\frac{a_1 - \tilde{\mu}}{\tilde{\sigma}}))} \exp\left(\frac{1}{8}x^4\tilde{\sigma}^2 - \frac{1}{2}\tilde{\mu}x^2\right) \operatorname{erfc}\left(\frac{\frac{1}{2}x^2\tilde{\sigma}^2 - \tilde{\mu}}{\sqrt{2}\tilde{\sigma}}\right) \\ &= \frac{1}{2(1 - \Phi(\frac{-\tilde{\mu}}{\tilde{\sigma}}))} \exp\left(\frac{1}{8}x^4\tilde{\sigma}^2 - \frac{1}{2}\tilde{\mu}x^2\right) \operatorname{erfc}\left(\frac{\frac{1}{2}x^2\tilde{\sigma}^2 - \tilde{\mu}}{\sqrt{2}\tilde{\sigma}}\right) \end{aligned}$$

where $\tilde{\mu} = \frac{ms^2}{n}$ and $\tilde{\sigma}^2 = m\sigma^2$. Hence we prove this Lemma. \square

Theorem A.3. *The collision probability of FastLSH is as follows:*

$$p(s, \sigma) = \Pr[h_{\tilde{a}, \tilde{b}}(\mathbf{v}) = h_{\tilde{a}, \tilde{b}}(\mathbf{u})] = \int_0^{\tilde{w}} f_{|\tilde{s}X|}(t) \left(1 - \frac{t}{\tilde{w}}\right) dt$$

Proof. Let $f_{|\tilde{s}X|}(t)$ represent the PDF of the absolute value of $\tilde{s}X$. For given bucket width \tilde{w} , the probability $p(|\tilde{s}X| < t)$ for any pair (\mathbf{v}, \mathbf{u}) is computed as $p(|\tilde{s}X| < t) = \int_0^{\tilde{w}} f_{|\tilde{s}X|}(t) dt$, where $t \in [0, \tilde{w}]$. Recall that \tilde{b} follows the uniform distribution $U(0, \tilde{w})$, the probability $p(\tilde{b} < \tilde{w} - t)$ is thus $(1 - \frac{t}{\tilde{w}})$. This means that after random projection, $(|\tilde{s}X| + \tilde{b})$ is also within the same bucket, and the collision probability $p(s, \sigma)$ is the product of $p(|\tilde{s}X| < t)$ and $p(\tilde{b} < \tilde{w} - t)$. Hence we prove this Theorem. \square

Theorem A.4.

$$\lim_{m \rightarrow +\infty} \frac{\varphi_{\tilde{s}X}(x)}{\exp(-\frac{ms^2x^2}{2n})} = 1$$

where $|x| \leq O(m^{-1/2})$ and $\exp(-\frac{ms^2x^2}{2n})$ is the characteristic function of $\mathcal{N}(0, \frac{ms^2}{n})$.

Proof. Recall that $\tilde{\mu} = \frac{ms^2}{n}$ and $\tilde{\sigma} = m\sigma^2$. $\varphi_{\tilde{s}X}(x)$ can be written as follows:

$$\varphi_{\tilde{s}X}(x) = \frac{1}{2(1 - \Phi(-\frac{\sqrt{ms^2}}{n\sigma}))} \exp\left(\frac{mx^4\sigma^2}{8} - \frac{ms^2x^2}{2n}\right) \operatorname{erfc}\left(\frac{\sqrt{m}(nx^2\sigma^2 - 2s^2)}{2\sqrt{2}n\sigma}\right) \quad (-\infty < x < +\infty)$$

Let $a = \frac{s^2}{\sqrt{2}n\sigma} > 0$ and $b = \frac{\sigma}{2\sqrt{2}} > 0 \Rightarrow b^2 = \frac{\sigma^2}{8}$. According to the fact $\Phi(x) = \frac{1}{2} \operatorname{erfc}(-\frac{x}{\sqrt{2}})$, $\varphi_{\tilde{s}X}(x)$ is simplified as:

$$\varphi_{\tilde{s}X}(x) = \exp(b^2mx^4 - \frac{1}{2}m\mu x^2) \cdot \frac{\operatorname{erfc}(b\sqrt{m}x^2 - a\sqrt{m})}{2 - \operatorname{erfc}(a\sqrt{m})}$$

Let $g(x) = \frac{\varphi_{\tilde{s}X}(x)}{\varphi_{sX}(x)}$, where $\varphi_{sX}(x) = \exp(-\frac{ms^2x^2}{2n})$ is the characteristic function of $\mathcal{N}(0, \frac{ms^2}{n})$. Then $g(x)$ is denoted as:

$$g(x) = \exp(b^2mx^4) \cdot \frac{\operatorname{erfc}(b\sqrt{m}x^2 - a\sqrt{m})}{2 - \operatorname{erfc}(a\sqrt{m})}$$

To prove $\varphi_{\tilde{s}X}(x) = \varphi_{sX}(x)$, we convert to prove whether $g(x) = 1$ as $m \rightarrow \infty$. Obviously $x^2 \leq O(m^{-1})$. Then $\sqrt{m}x^2 \leq O(m^{-1/2})$ and $mx^4 \leq O(m^{-1})$. It is easy to derive:

$$\lim_{m \rightarrow +\infty} \exp(b^2mx^4) = 1$$

It holds for any fixed $b \in \mathbb{R}^+$. On the other hand, we have:

$$\operatorname{erfc}(b\sqrt{m}x^2 - a\sqrt{m}) \sim \operatorname{erfc}(-a\sqrt{m}), \quad m \rightarrow +\infty$$

Actually using the fact $b\sqrt{m}x^2 - a\sqrt{m} \sim -a\sqrt{m}$ as $m \rightarrow +\infty$ and $\operatorname{erfc}(-x) = 2 - \frac{\exp(-x^2)}{\sqrt{\pi x}}$ as $x \rightarrow +\infty$, we have:

$$\lim_{m \rightarrow +\infty} \frac{\operatorname{erfc}(b\sqrt{m}x^2 - a\sqrt{m})}{2 - \operatorname{erfc}(a\sqrt{m})} = \frac{\lim_{m \rightarrow +\infty} \operatorname{erfc}(b\sqrt{m}x^2 - a\sqrt{m})}{\lim_{m \rightarrow +\infty} \operatorname{erfc}(-a\sqrt{m})} = 1$$

Hence we have:

$$g(x) = \lim_{m \rightarrow +\infty} \exp(b^2mx^4) \cdot \lim_{m \rightarrow +\infty} \frac{\operatorname{erfc}(b\sqrt{m}x^2 - a\sqrt{m})}{\operatorname{erfc}(-a\sqrt{m})} = 1.$$

\square

If the characteristic function of a random variable Z exists, it provides a way to compute its various moments. Specifically, the r -th moment of Z denoted by $E(Z^r)$ can be expressed as the r -th derivative of the characteristic function evaluated at zero (Hoel et al., 1971), i.e.,

$$E(Z^r) = (i)^{-r} \frac{d^r}{dt^r} \varphi_Z(t) \Big|_{t=0} \quad (10)$$

where $\varphi_Z(t)$ denotes the characteristic function of Z . If we know the characteristic function, then all of the moments of the random variable Z can be obtained.

Lemma A.5.

$$\begin{cases} E(\tilde{s}X) = 0 \\ E((\tilde{s}X)^2) = \frac{ms^2}{n}(1 + \epsilon) \\ E((\tilde{s}X)^3) = 0 \\ E((\tilde{s}X)^4) = \frac{3m^2s^4}{n^2}(1 + \lambda) \end{cases}$$

where $\epsilon = \frac{\tilde{\sigma} \exp(\frac{-\tilde{\mu}^2}{2\tilde{\sigma}^2})}{\sqrt{2\pi}\tilde{\mu}(1-\Phi(\frac{-\tilde{\mu}}{\tilde{\sigma}}))}$ and $\lambda = \frac{\tilde{\sigma}^2}{\tilde{\mu}^2} + \epsilon$.

Proof. From Lemma A.2, we can easily compute the first-order derivative of characteristic function with respect to x , which is as follows:

$$\varphi'_{\tilde{s}X}(x) = \frac{\exp(\frac{1}{8}x^4\tilde{\sigma}^2 - \frac{1}{2}\tilde{\mu}x^2)}{2(1 - \Phi(\frac{-\tilde{\mu}}{\tilde{\sigma}}))} \left[\left(\frac{1}{2}x^3\tilde{\sigma}^2 - \tilde{\mu}x \right) \operatorname{erfc}\left(\frac{\frac{1}{2}x^2\tilde{\sigma}^2 - \tilde{\mu}}{\sqrt{2}\tilde{\sigma}}\right) - \frac{2\tilde{\sigma}x}{\sqrt{2\pi}} \exp\left(-\left(\frac{\frac{1}{2}x^2\tilde{\sigma}^2 - \tilde{\mu}}{\sqrt{2}\tilde{\sigma}}\right)^2\right) \right] \quad (11)$$

Then the second-order derivative is

$$\begin{aligned} \varphi''_{\tilde{s}X}(x) = & \frac{\exp(\frac{1}{8}x^4\tilde{\sigma}^2 - \frac{1}{2}\tilde{\mu}x^2)}{2(1 - \Phi(\frac{-\tilde{\mu}}{\tilde{\sigma}}))} \left[\left(\left(\frac{1}{2}x^3\tilde{\sigma}^2 - ux \right)^2 + \frac{3}{2}x^2\tilde{\sigma}^2 - \tilde{\mu} \right) \operatorname{erfc}\left(\frac{\frac{1}{2}x^2\tilde{\sigma}^2 - \tilde{\mu}}{\sqrt{2}\tilde{\sigma}}\right) \right. \\ & \left. - \frac{2}{\sqrt{2\pi}} \left(\tilde{\sigma} + \frac{3}{2}x^4\tilde{\sigma}^3 - \frac{3}{2}\tilde{\mu}\tilde{\sigma}x^2 \right) \exp\left(-\left(\frac{\frac{1}{2}x^2\tilde{\sigma}^2 - \tilde{\mu}}{\sqrt{2}\tilde{\sigma}}\right)^2\right) \right] \end{aligned} \quad (12)$$

The third-order derivative is

$$\begin{aligned} \varphi'''(x) = & \frac{\exp(\frac{1}{8}x^4\tilde{\sigma}^2 - \frac{1}{2}\tilde{\mu}x^2)}{2(1 - \Phi(\frac{-\tilde{\mu}}{\tilde{\sigma}}))} \left[\left(\frac{1}{8}\tilde{\sigma}^6x^9 - \frac{3}{4}\tilde{\mu}\tilde{\sigma}^4x^7 + \left(\frac{2}{3}\tilde{\mu}^2\tilde{\sigma}^2 + \frac{9}{4}\tilde{\sigma}^4 \right)x^5 - (6\tilde{\mu}\tilde{\sigma}^2 + \tilde{\mu}^3)x^3 + 3(\tilde{\mu}^2 + \tilde{\sigma}^2)x \right) \right. \\ & \left. \operatorname{erfc}\left(\frac{\frac{1}{2}\tilde{\sigma}^2x^2 - \tilde{\mu}}{\sqrt{2}\tilde{\sigma}}\right) - \frac{2}{\sqrt{2\pi}} \left(\frac{1}{4}\tilde{\sigma}^5x^7 - \tilde{\mu}\tilde{\sigma}^3x^5 + (\tilde{\mu}^2\tilde{\sigma} + \frac{7}{2}\tilde{\sigma}^3)x^3 - 3\tilde{\mu}\tilde{\sigma}x \right) \exp\left(-\left(\frac{\frac{1}{2}\tilde{\sigma}^2x^2 - \tilde{\mu}}{\sqrt{2}\tilde{\sigma}}\right)^2\right) \right] \end{aligned} \quad (13)$$

The fourth-order derivative is

$$\begin{aligned} \varphi''''(x) = & \frac{\exp(\frac{1}{8}x^4\tilde{\sigma}^2 - \frac{1}{2}\tilde{\mu}x^2)}{2(1 - \Phi(\frac{-\tilde{\mu}}{\tilde{\sigma}}))} \left[\left(\frac{1}{16}\tilde{\sigma}^8x^{12} - \frac{1}{2}\tilde{\mu}\tilde{\sigma}^6x^{10} + \left(\frac{3}{2}\tilde{\mu}^2\tilde{\sigma}^4 + \frac{9}{4}\tilde{\sigma}^4 \right)x^8 - (2\tilde{\mu}^3\tilde{\sigma}^2 + \frac{21}{2}\tilde{\mu}\tilde{\sigma}^4)x^6 \right. \right. \\ & \left. \left. + (\tilde{\mu}^4 + \frac{51}{4}\tilde{\sigma}^4 + 9\tilde{\mu}^2\tilde{\sigma}^2)x^4 - (6\tilde{\mu}^3 + 21\tilde{\mu}\tilde{\sigma}^2)x^2 + 3(\tilde{\mu}^2 + \tilde{\sigma}^2) \right) \operatorname{erfc}\left(\frac{\frac{1}{2}\tilde{\sigma}^2x^2 - \tilde{\mu}}{\sqrt{2}\tilde{\sigma}}\right) \right. \\ & \left. - \frac{2}{\sqrt{2\pi}} \left(\frac{1}{8}\tilde{\sigma}^7x^{10} - \frac{3}{4}\tilde{\mu}\tilde{\sigma}^5x^8 + \left(\frac{3}{2}\tilde{\mu}^2\tilde{\sigma}^3 + 4\tilde{\sigma}^5 \right)x^6 - (6\tilde{\mu}^2\tilde{\sigma} + \frac{13}{2}\tilde{\sigma}^3)x^2 - 3\tilde{\mu}\tilde{\sigma} \right) \exp\left(-\left(\frac{\frac{1}{2}\tilde{\sigma}^2x^2 - \tilde{\mu}}{\sqrt{2}\tilde{\sigma}}\right)^2\right) \right] \end{aligned} \quad (14)$$

Let $E(\tilde{s}X - E(\tilde{s}X))^i$ for $i \in \{1, 2, 3, 4\}$ denote the first four central moments. According to Eqn. (10), we know that $E(\tilde{s}X) = \frac{\varphi'(0)}{i} = 0$, then it is easy to derive $E(\tilde{s}X - E(\tilde{s}X))^i = E((\tilde{s}X)^i)$. To this end, by Eqn. (11) - (14), we have the following results:

$$\begin{cases} E(\tilde{s}X) = 0 \\ E((\tilde{s}X)^2) = \frac{\tilde{\mu} \operatorname{erfc}(\frac{-\tilde{\mu}}{\sqrt{2}\tilde{\sigma}}) + \frac{2\tilde{\sigma}}{\sqrt{2\pi}} \exp(\frac{-\tilde{\mu}^2}{2\tilde{\sigma}^2})}{2(1 - \Phi(\frac{-\tilde{\mu}}{\tilde{\sigma}}))} \\ E((\tilde{s}X)^3) = 0 \\ E((\tilde{s}X)^4) = \frac{3(\tilde{\mu}^2 + \tilde{\sigma}^2) \operatorname{erfc}(\frac{-\tilde{\mu}}{\sqrt{2}\tilde{\sigma}}) + \frac{6\tilde{\mu}\tilde{\sigma}}{\sqrt{2\pi}} \exp(\frac{-\tilde{\mu}^2}{2\tilde{\sigma}^2})}{2(1 - \Phi(\frac{-\tilde{\mu}}{\tilde{\sigma}}))} \end{cases} \quad (15)$$

where $E(\tilde{s}X)$ is the expectation; $E((\tilde{s}X)^2)$ is the variance; $\frac{E((\tilde{s}X)^3)}{(E((\tilde{s}X)^2))^{\frac{3}{2}}}$ is the skewness; $\frac{E((\tilde{s}X)^4)}{(E((\tilde{s}X)^2))^2}$ is the kurtosis. Since

$$\frac{\operatorname{erfc}\left(\frac{-\tilde{\mu}}{\sqrt{2\tilde{\sigma}}}\right)}{2(1 - \Phi\left(\frac{-\tilde{\mu}}{\tilde{\sigma}}\right))} = \frac{\frac{2}{\sqrt{\pi}} \int_{\frac{-\tilde{\mu}}{\sqrt{2\tilde{\sigma}}}^+}{+\infty} \exp(-t_1^2) dt_1}{2(1 - \frac{1}{\sqrt{2\pi}} \int_{-\infty}^{\frac{-\tilde{\mu}}{\tilde{\sigma}}} \exp(\frac{-t_2^2}{2}) dt_2)} = \frac{\int_{\frac{-\tilde{\mu}}{\sqrt{2\tilde{\sigma}}}^+}{+\infty} \exp(-t_1^2) dt_1}{\sqrt{2} \int_{\frac{-\tilde{\mu}}{\tilde{\sigma}}}^{+\infty} \exp(\frac{-t_2^2}{2}) dt_2} = \frac{\int_{\frac{-\tilde{\mu}}{\sqrt{2\tilde{\sigma}}}^+}{+\infty} \exp(-t_1^2) dt_1}{\int_{\frac{-\tilde{\mu}}{\sqrt{2\tilde{\sigma}}}^+}{+\infty} \exp(-t^2) dt} = 1$$

Therefore, Eqn. (15) can be rewritten as below

$$\begin{cases} E(\tilde{s}X) = 0 \\ E((\tilde{s}X)^2) = \tilde{\mu}(1 + \epsilon) \\ E((\tilde{s}X)^3) = 0 \\ E((\tilde{s}X)^4) = 3\tilde{\mu}^2(1 + \lambda) \end{cases}$$

where $\epsilon = \frac{\tilde{\sigma} \exp(\frac{-\tilde{\mu}^2}{2\tilde{\sigma}^2})}{\sqrt{2\pi}\tilde{\mu}(1 - \Phi(\frac{-\tilde{\mu}}{\tilde{\sigma}}))}$, $\lambda = \frac{\tilde{\sigma}^2}{\tilde{\mu}^2} + \epsilon$, $\tilde{\mu} = \frac{m\tilde{s}^2}{n}$ and $\tilde{\sigma}^2 = m\sigma^2$. We prove this Lemma. \square

B. Extension to Maximum Inner Product Search

(Bachrach et al., 2014; Shrivastava & Li, 2014a) shows that there exists two transformation functions, by which the maximum inner product search (MIPS) problem can be converted into solve the near neighbor search problem. More specifically, the two transformation functions are $P(\mathbf{v}) = (\sqrt{\kappa^2 - \|\mathbf{v}\|_2^2}, \mathbf{v})$ for data processing and $Q(\mathbf{u}) = (0, \mathbf{u})$ for query processing respectively, where $\kappa = \max(\|\mathbf{v}_i\|_2)$ ($i \in \{1, 2, \dots, N\}$). Then the relationship between maximum inner product and l_2 norm for any vector pair $(\mathbf{v}_i, \mathbf{u})$ is denoted as $\operatorname{argmax}_i(\frac{P(\mathbf{v}_i)Q(\mathbf{u})}{\|P(\mathbf{v}_i)\|_2\|Q(\mathbf{u})\|_2}) = \operatorname{argmin}_i(\|\mathbf{v}_i - \mathbf{u}\|_2)$ for $\|\mathbf{u}\|_2 = 1$.

To make FastLSH applicable for MIPS, we first apply the sample operator $S(\cdot)$ defined earlier to vector pairs $(\mathbf{v}_i, \mathbf{u})$ for yielding $\tilde{\mathbf{v}}_i = S(\mathbf{v}_i)$ and $\tilde{\mathbf{u}} = S(\mathbf{u})$, and then obtain $\tilde{P}(\mathbf{v}) = (\sqrt{\tilde{\kappa}^2 - \|S(\mathbf{v})\|_2^2}, S(\mathbf{v}))$ and $\tilde{Q}(\mathbf{u}) = (0, S(\mathbf{u}))$, where $\tilde{\kappa} = \max(\|S(\mathbf{v}_i)\|_2)$ is a constant. Then $\operatorname{argmax}_i(\frac{\tilde{P}(\mathbf{v}_i)\tilde{Q}(\mathbf{u})}{\|\tilde{P}(\mathbf{v}_i)\|_2\|\tilde{Q}(\mathbf{u})\|_2}) = \operatorname{argmin}_i(\|\tilde{\mathbf{v}}_i - \tilde{\mathbf{u}}\|_2)$ for $\|S(\mathbf{u})\|_2 = 1$. Let $\Delta = \tilde{\kappa}^2 - \|S(\mathbf{v})\|_2^2$. After random projection, $\mathbf{a}^T \tilde{P}(\mathbf{v}) - \mathbf{a}^T \tilde{Q}(\mathbf{u})$ is distributed as $(\sqrt{\tilde{s}^2 + \Delta})X$. Since $\tilde{s}^2 \sim \mathcal{N}(m\mu, m\sigma^2)$, then $(\tilde{s}^2 + \Delta) \sim \mathcal{N}(m\mu + \Delta, m\sigma^2)$. Let $\sqrt{\tilde{s}^2 + \Delta}$ be the random variable \mathcal{I} . Similar to Eqn. (7), the PDF of \mathcal{I} represented by $f_{\mathcal{I}}$ is yielded as follow:

$$f_{\mathcal{I}}(t) = 2t\psi(t^2; m\mu + \Delta, m\sigma^2, 0, +\infty) \quad (16)$$

By applying Lemma A.1, the characteristic function of $\mathcal{I}X$ is as follows:

$$\varphi_{\mathcal{I}X}(x) = \frac{1}{2(1 - \Phi(\frac{-m\sigma^2 - n\Delta}{\sqrt{m\sigma\Delta}}))} \exp\left(\frac{mx^4\sigma^2}{8} - \frac{(ms^2 + n\Delta)x^2}{2n}\right) \operatorname{erfc}\left(\frac{mnx^2\sigma^2 - 2(ms^2 + n\Delta)}{2\sqrt{2mn}\sigma}\right) (-\infty < x < +\infty) \quad (17)$$

Then the PDF of $\mathcal{I}X$ is obtained by $\varphi_{\mathcal{I}X}(x)$:

$$f_{\mathcal{I}X}(t) = \frac{1}{2\pi} \int_{-\infty}^{\infty} \varphi_{\mathcal{I}X}(x) \exp(-itx) dx \quad (18)$$

It is easy to derive the collision probability of any pair (\mathbf{v}, \mathbf{u}) by $f_{\mathcal{I}X}(t)$, which is as follows:

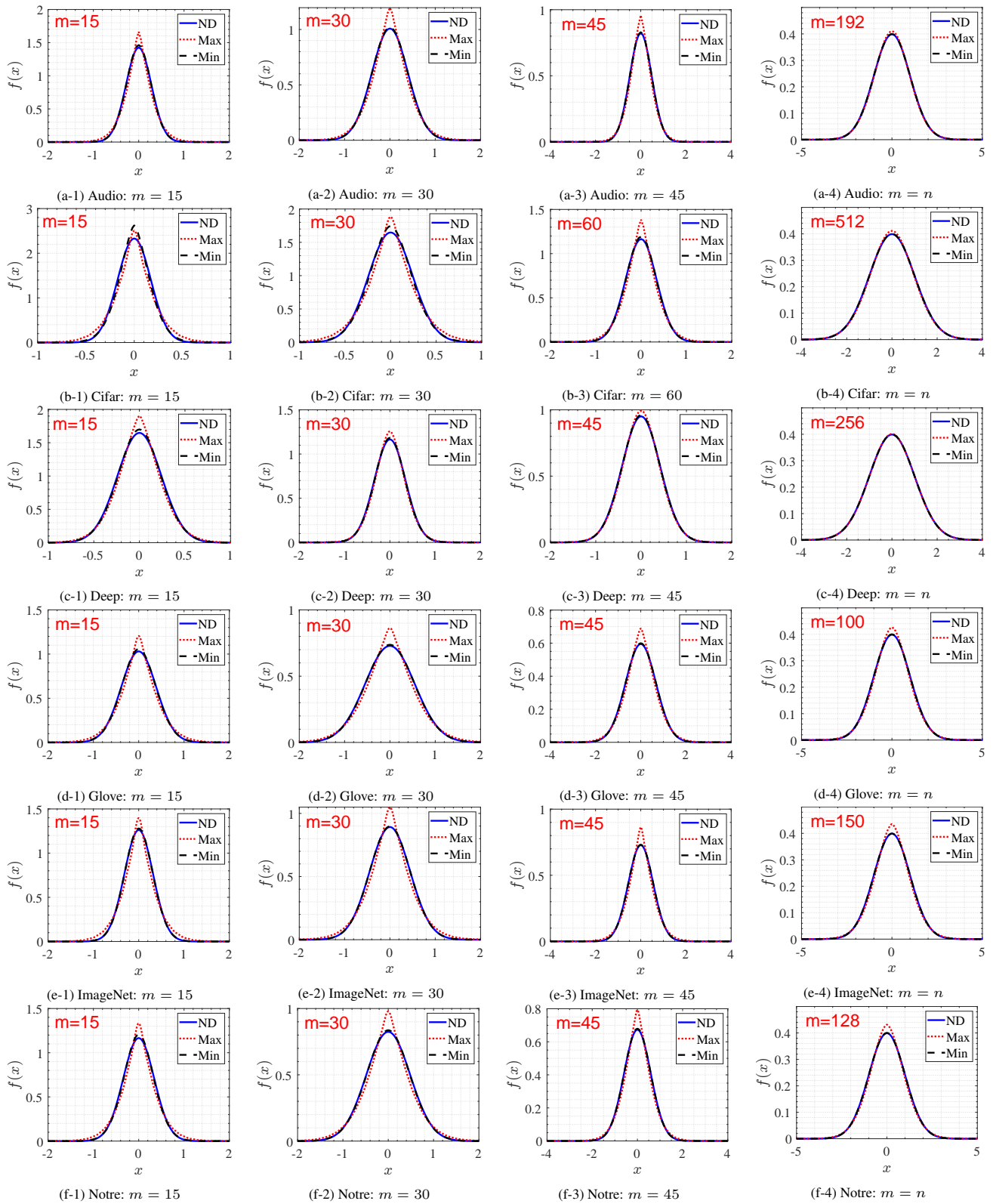
$$p(s) = \int_0^{\tilde{w}'} f_{|\mathcal{I}X|}(t) \left(1 - \frac{t}{\tilde{w}'}\right) dx \quad (19)$$

where $f_{|\mathcal{I}X|}(t)$ denotes the PDF of the absolute value of $\mathcal{I}X$. \tilde{w}' is the bucket width.

C. Additional Experiments

Table 2. ϵ and λ for different m

Datasets		$m = 15$		$m = 30$		$m = 45/60$		$m = n$	
		ϵ	λ	ϵ	λ	ϵ	λ	ϵ	λ
Cifar	max	0.567575	2.527575	0.287600	1.287600	0.114125	0.618225	0.000064	0.067664
	mean	0.102716	0.575372	0.027539	0.277239	0.001994	0.120123	0	0.014617
	min	0.019616	0.239671	0.001702	0.116014	0.000011	0.055001	0	0.006691
Sun	max	0.502360	2.218460	0.236626	1.084867	0.095099	0.546683	0.000006	0.051535
	mean	0.022783	0.255107	0.001849	0.118130	0.000018	0.058099	0	0.006724
	min	0	0.040401	0	0.020736	0	0.010000	0	0.001156
Gist	max	0.633640	2.853740	0.274502	1.234902	0.129940	0.677540	0	0.032400
	mean	0.042122	0.340238	0.005183	0.152639	0.000133	0.074662	0	0.004624
	min	0.000064	0.067664	0	0.038025	0	0.016926	0	0.001089
Trevi	max	0.013420	0.207020	0.001105	0.106081	0.000003	0.049287	0	0.000729
	mean	0.000011	0.055236	0	0.029241	0	0.013924	0	0.000196
	min	0	0.015876	0	0.008100	0	0.003969	0	0.000100
Audio	max	0.268000	1.208900	0.099004	0.561404	0.043520	0.346020	0.000033	0.062533
	mean	0.033344	0.303017	0.003637	0.138767	0.000480	0.091021	0	0.020967
	min	0.000022	0.059705	0	0.030765	0	0.021874	0	0.005329
Notre	max	0.341109	1.507509	0.143598	0.728823	0.074226	0.467355	0.004017	0.142401
	mean	0.022783	0.255107	0.001902	0.118866	0.000172	0.077456	0	0.027225
	min	0.000101	0.071925	0	0.036481	0	0.023716	0	0.008281
Glove	max	0.261530	1.183130	0.094131	0.543031	0.040065	0.331665	0.002362	0.124862
	mean	0.003190	0.134234	0.000047	0.065072	0.000001	0.043265	0	0.019853
	min	0.000025	0.060541	0	0.029929	0	0.020335	0	0.009409
Sift	max	0.294194	1.314294	0.098513	0.559554	0.057014	0.400410	0.001296	0.109537
	mean	0.054265	0.389506	0.007185	0.167986	0.001509	0.113065	0	0.036864
	min	0.003755	0.139916	0.000107	0.072468	0.000001	0.045370	0	0.016129
Deep	max	0.036744	0.317644	0.003841	0.140741	0.000463	0.090463	0	0.014400
	mean	0.003047	0.132719	0.000044	0.064560	0.000001	0.043306	0	0.007569
	min	0.000199	0.079160	0	0.039204	0	0.026374	0	0.004638
Random	max	0.077344	0.479300	0.015195	0.216796	0.003505	0.137461	0.000041	0.064050
	mean	0.002824	0.130273	0.000038	0.063542	0.000001	0.042437	0	0.019044
	min	0.000024	0.060049	0	0.029929	0.	0.019881	0	0.008649
Ukbench	max	0.692955	3.157855	0.361581	1.593681	0.217238	1.009338	0.039727	0.330248
	mean	0.139183	0.712232	0.034502	0.308031	0.012672	0.202768	0.000056	0.066620
	min	0.002895	0.131059	0.000041	0.064050	0.000001	0.042437	0	0.015376
ImageNet	max	0.466568	2.054168	0.217238	1.009338	0.119323	0.637723	0.004773	0.149173
	mean	0.019125	0.237214	0.001336	0.110236	0.000107	0.072468	0	0.022201
	min	0	0.033489	0	0.016641	0	0.011025	0	0.003481



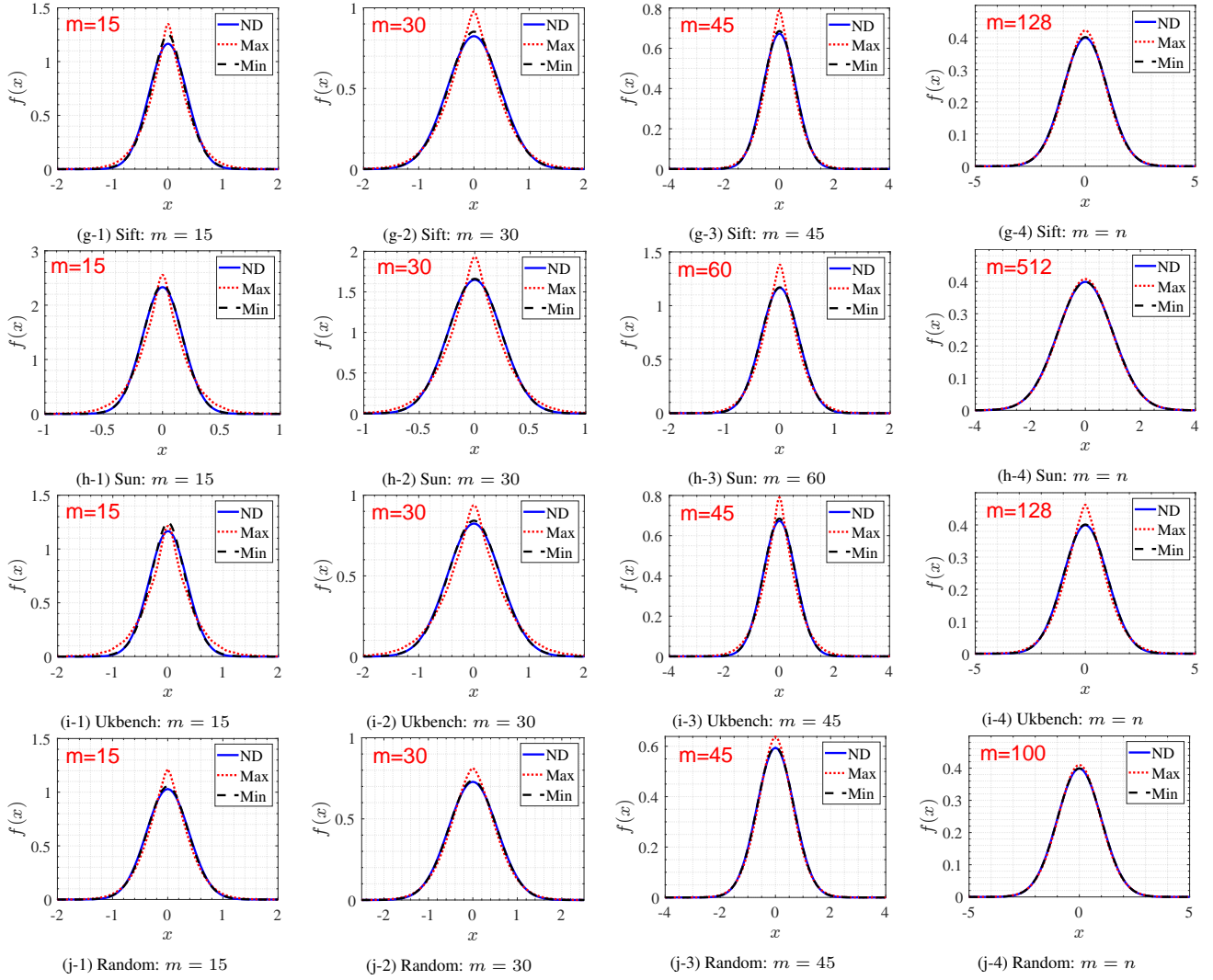


Figure 4. Comparison of probability density curves of $\mathcal{N}(0, \frac{ms^2}{n})$ (ND) and $\tilde{s}X$ under different m .

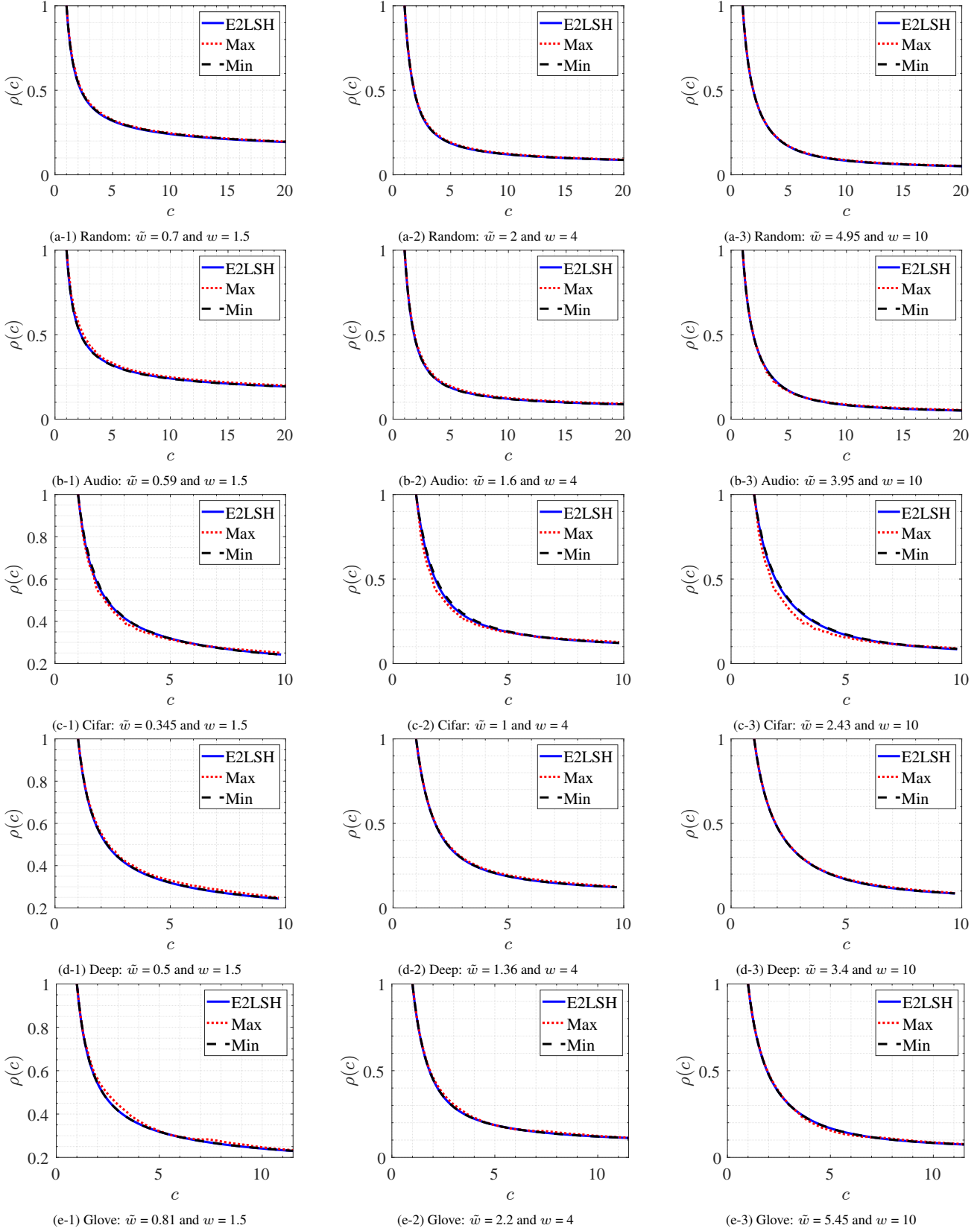


Figure 5. ρ curves under different bucket widths over datasets *Random*, *Audio* and *Cifar*, *Deep* and *Glove*.

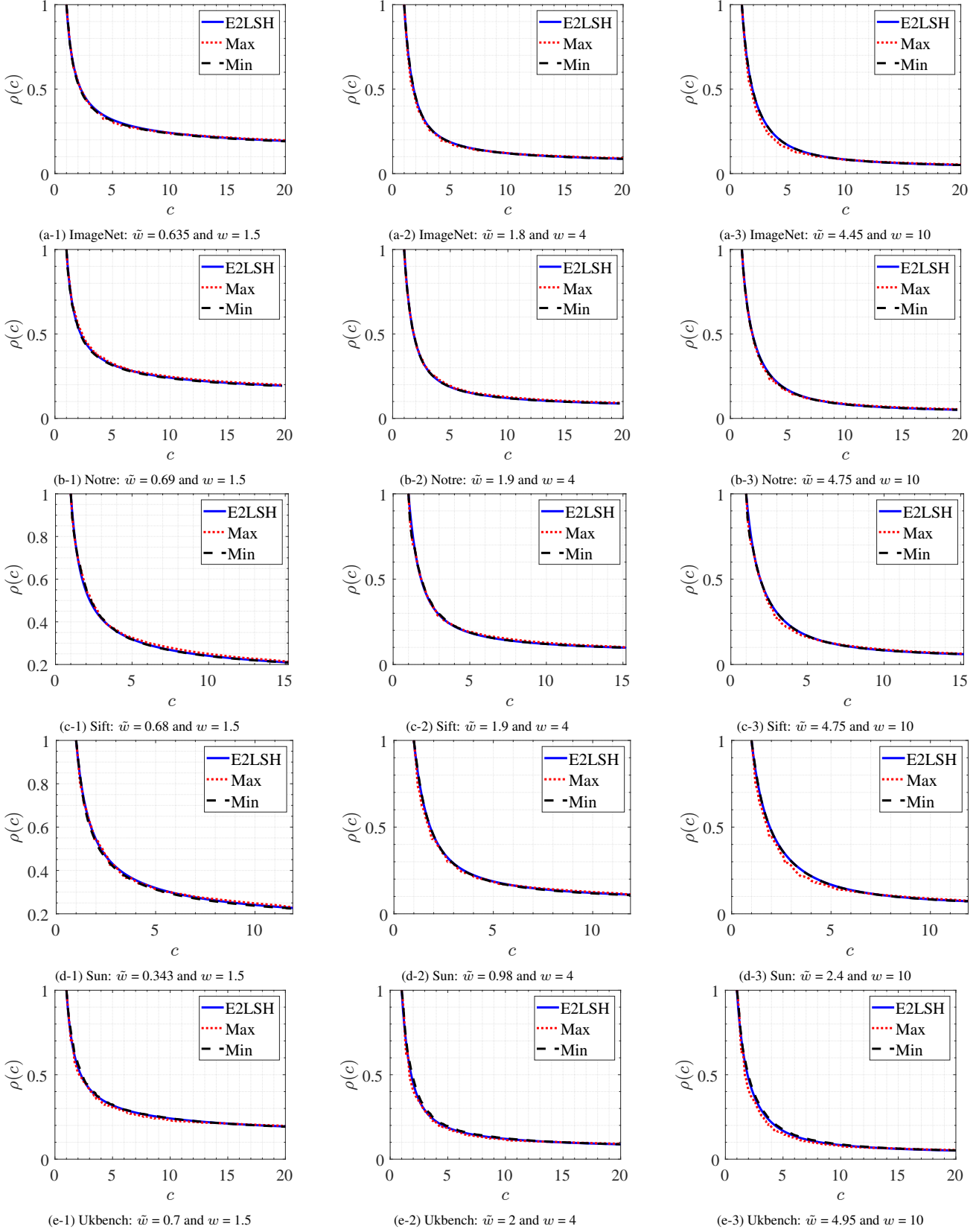


Figure 6. ρ curves under different bucket widths over datasets *ImageNet*, *Notre*, *Sift*, *Sun* and *Ukbench*.

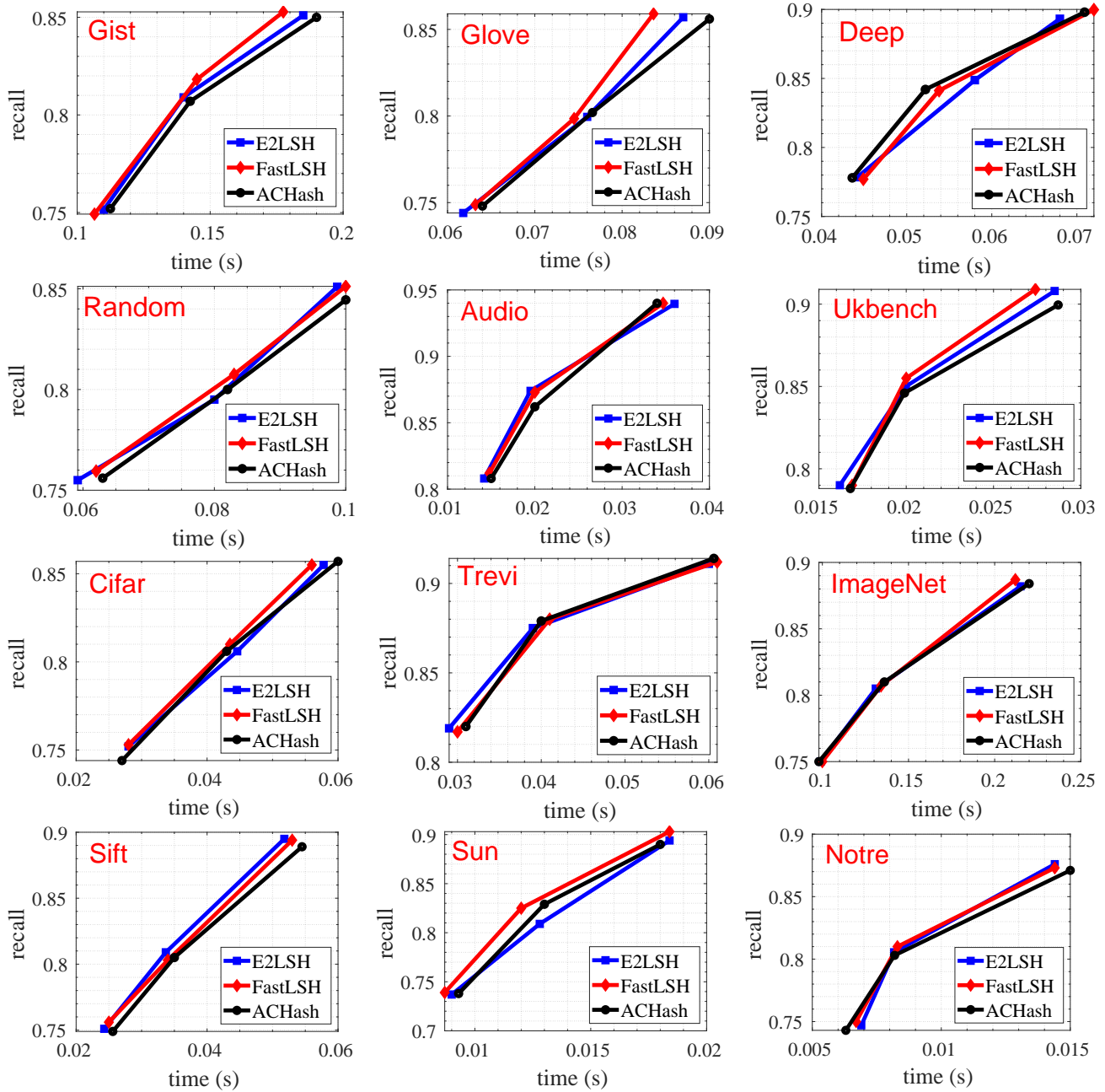


Figure 7. Recall v.s. average query time